

Organic Super-Acceptors with Efficient Intramolecular Charge-Transfer Interactions by [2+2] Cycloadditions of TCNE, TCNQ, and F₄-TCNQ to Donor-Substituted Cyanoalkynes**

Milan Kivala,^[a] Corinne Boudon,^[b] Jean-Paul Gisselbrecht,^[b] Barbara Enko,^[c]
Paul Seiler,^[a] Imke B. Müller,^[d] Nicolle Langer,^[d] Peter D. Jarowski,^[a]
Georg Gescheidt,^[c] and François Diederich*^[a]

Dedicated to Professor Seiji Shinkai on the occasion of his 65th birthday

Abstract: Thermal [2+2] cycloadditions of tetracyanoethene (TCNE), 7,7,8,8-tetracyanoquinodimethane (TCNQ), and 2,3,5,6-tetrafluoro-7,7,8,8-tetracyanoquinodimethane (F₄-TCNQ) to *N,N*-dimethylanilino-substituted (DMA-substituted) alkynes bearing either nitrile, dicyanovinyl (DCV; -CH=C(CN)₂), or tricyanovinyl (TCV; -C(CN)=C(CN)₂) functionalities, followed by retro-electrocyclization, afforded a new class of stable organic super-acceptors. Despite the non-planarity of these acceptors, as revealed by X-ray crystallographic analysis and theoretical calculations, efficient intramolecular charge-transfer (CT) interactions between the DMA donors and the CN-containing acceptor moieties are established. The corresponding CT bands appear strongly bathochromically shifted with maxima up to 1120 nm (1.11 eV) accompanied by an end-absorption in the near infrared around 1600 nm (0.78 eV) for F₄-TCNQ adducts. Electronic absorp-

tion spectra of selected acceptors were nicely reproduced by applying the spectroscopy oriented configuration interaction (SORCI) procedure. The electrochemical investigations of these acceptors by cyclic voltammetry (CV) and rotating disc voltammetry (RDV) in CH₂Cl₂ identified their remarkable propensity for reversible electron uptake rivaling the benchmark compounds TCNQ ($E_{\text{red},1} = -0.25$ V in CH₂Cl₂ vs. Fc⁺/Fc) and F₄-TCNQ ($E_{\text{red},1} = +0.16$ V in CH₂Cl₂ vs. Fc⁺/Fc). Furthermore, the electron-accepting power of these new compounds expressed as adiabatic electron affinity (EA) has been estimated by theoretical calculations and compared to the reference acceptor F₄-TCNQ, which is used as a p-type dopant in the fabrication of

organic light-emitting diodes (OLEDs) and solar cells. A good linear correlation exists between the calculated EAs and the first reduction potentials $E_{\text{red},1}$. Despite the substitution with strong DMA donors, the predicted EAs reach the value calculated for F₄-TCNQ (4.96 eV) in many cases, which makes the new acceptors interesting for potential applications as dopants in organic optoelectronic devices. The first example of a charge-transfer salt between the DMA-substituted TCNQ adduct ($E_{\text{red},1} = -0.27$ V vs. Fc⁺/Fc) and the strong electron donor decamethylferrocene ([FcCp*]₂); Cp* = pentamethylcyclopentadienide; $E_{\text{ox},1} = -0.59$ V vs. Fc⁺/Fc) is described. Interestingly, the X-ray crystal structure showed that in the solid state the TCNQ moiety in the acceptor underwent reductive σ -dimerization upon reaction with the donor.

Keywords: charge transfer • cycloaddition • electrochemistry • electron acceptors • electron affinity • EPR spectroscopy

[a] Dr. M. Kivala, P. Seiler, Dr. P. D. Jarowski, Prof. Dr. F. Diederich
Laboratorium für Organische Chemie
ETH Zürich
Hönggerberg, HCI, 8093 Zürich (Switzerland)
Fax: (+41)44 632 1109
E-mail: diederich@org.chem.ethz.ch

[b] Prof. Dr. C. Boudon, Dr. J.-P. Gisselbrecht
Laboratoire d'Electrochimie et de Chimie Physique du Corps Solide
Institut de Chimie—UMR 7177, CNRS, Université Louis Pasteur
4, rue Blaise Pascal, 67000, Strasbourg (France)

[c] B. Enko, Prof. Dr. G. Gescheidt
Institut für Physikalische und Theoretische Chemie, TU Graz
Technikerstrasse 4/I, 8010 Graz (Austria)

[d] Dr. I. B. Müller, Dr. N. Langer
BASF SE, GVP/C—A030, 67056 Ludwigshafen (Germany)

[**] TCNE = tetracyanoethene, TCNQ = 7,7,8,8-tetracyanoquinodimethane, F₄-TCNQ = 2,3,5,6-tetrafluoro-7,7,8,8-tetracyanoquinodimethane.

 Supporting information for this article is available on the WWW under <http://dx.doi.org/10.1002/chem.200802563>.

Introduction

Among the large number of strong organic acceptors that have been described to date, cyano-based derivatives represent the most prominent class of compounds for optoelectronic device applications.^[1] Tetracyanoethene (TCNE)^[2,3] and 7,7,8,8-tetracyanoquinodimethane (TCNQ)^[4,5] together with their derivatives^[6] were shown to form charge-transfer (CT) complexes and salts with various organic and organometallic electron donors that often exhibit technologically interesting materials properties such as electric conductivity^[7,8] and magnetic phenomena.^[9] Furthermore, environmentally stable acceptors are increasingly applied as p-type dopants, significantly improving the performance of optoelectronic devices such as organic light-emitting diodes (OLEDs) and solar cells.^[10] Although 2,3,5,6-tetrafluoro-7,7,8,8-tetracyanoquinodimethane (F₄-TCNQ)^[6a] is widely used for this purpose, alternative dopants, such as the recently reported 3,6-difluoro-2,5,7,7,8,8-hexacyanoquinodimethane (F₂-HCNQ) with superior thermal stability,^[11] are currently being pursued by many researchers.

Recently, we have shown that formal [2+2] cycloadditions, followed by retro-electrocyclization of the initially formed cyclobutenes, of TCNE^[12,13] and TCNQ^[14,15] to “electronically confused” alkynes bearing one electron-donating group and one electron-withdrawing group, such as *N,N*-dimethylanilino-substituted (DMA-substituted) cyanoalkynes, yield donor-substituted 1,1,2,4,4-pentacyanobuta-1,3-dienes^[16] (PCBDs) and the corresponding cyclohexa-2,5-diene-1,4-diyliene-expanded derivative, respectively.^[17] Despite the substitution with DMA donors, these compounds are potent electron acceptors that compete with TCNE and TCNQ in their ease of reversible electron uptake. Furthermore, intense bathochromically shifted intramolecular CT bands are observed in their UV/Vis spectra. Based on these results, we expected that even stronger electron acceptors would be in reach upon i) incorporation of particularly strong acceptor moieties, such as F₄-TCNQ, and ii) increasing the number of electron-withdrawing cyano functionalities in the molecule.

Here, we introduce a new family of strong electron acceptors **1–7** obtained by reactions of TCNE, TCNQ, and F₄-TCNQ with DMA-substituted alkynes bearing either nitrile (**8**),^[17,18] dicyanovinyl (DCV; -CH=C(CN)₂) (**9**),^[13b] or tricyanovinyl (TCV; -C(CN)=C(CN)₂) (**10**) functionalities (Table 1).^[19] Initial attempts to prepare intermolecular CT complexes with strong electron donors, such as decamethylferrocene ([FeCp*₂]; Cp* = pentamethylcyclopentadienide)^[20] will be discussed as well.

Results and Discussion

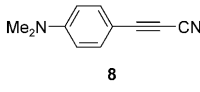
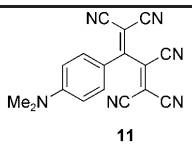
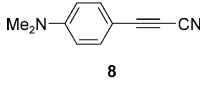
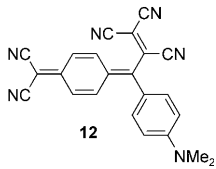
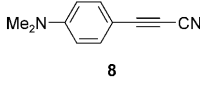
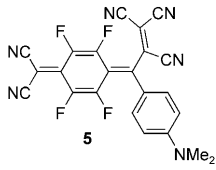
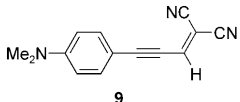
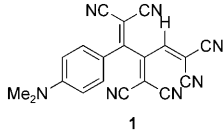
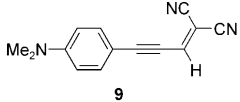
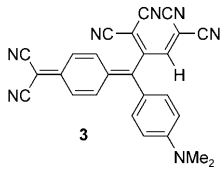
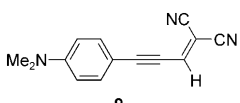
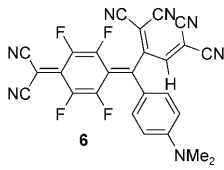
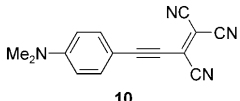
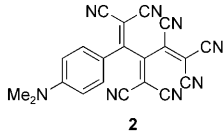
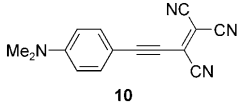
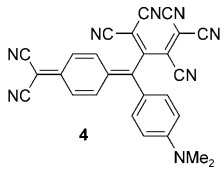
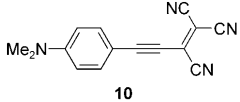
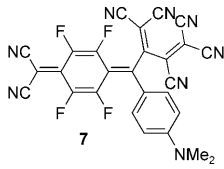
Synthesis and characterization: Whereas the previously reported reaction of TCNE with cyanoalkyne **8** to give DMA-substituted PCBD **11** proceeded in nearly quantitative yield in tetrahydrofuran (THF) at 20 °C,^[17] similar reaction with

DCV-substituted alkyne **9** and TCV-derivative **10** to yield the corresponding adducts **1** (26%) and **2** (66%), respectively, required heating in 1,2-dichloroethane or 1,1,4,4-tetrachloroethane up to 120 °C (Table 1). As already observed for **12**,^[17] TCNQ displays rather reduced reactivity, compared to TCNE, towards formal cycloadditions with alkynes. While an excess of TCNQ, prolonged reaction times, and elevated temperature (60 °C) were applied in the synthesis of **3**, complete consumption of the starting alkyne **9** could not be reached. Subsequent repeated chromatographic purifications on SiO₂ afforded **3** in a rather low yield of 14% due to partial decomposition during column chromatography (CC). Furthermore, reaction of TCNQ with TCV-substituted alkyne **10** under various conditions delivered only a trace amount of the corresponding heptacyano derivative **4**, accompanied by a mixture of unidentifiable products, as revealed by mass spectrometry. Gratifyingly, the stronger acceptor F₄-TCNQ showed significantly higher reactivity, compared to TCNQ, towards regioselective cycloadditions with alkynes. Thus, fluorinated adducts **5–7** were obtained in good yields ranging from 65 (**5**) to 88% (**7**), respectively, upon reaction with DMA-substituted cyanoalkynes **8–10** in CH₂Cl₂ at 25 °C (Table 1).

All newly prepared acceptors **1–3** and **5–7** are dark metallic-like solids that are stable at ambient temperature under air and reasonably soluble in common organic solvents such as CH₂Cl₂, acetone, and acetonitrile (except for nearly insoluble **6**). However, solutions of F₄-TCNQ adducts **5–7** were found to deteriorate gradually upon contact with glass surfaces to form green insoluble products. Thus, glassware previously deactivated by silylation with dimethyldichlorosilane (DMDCS) should be used for all manipulations involving **5–7**.^[21] Complete decomposition was observed during attempted chromatography (SiO₂ and C₁₈-reversed phase SiO₂) of **2** and **5–7**. Consequently, **2** and **5–7** were successfully purified by repeated crystallization by slow diffusion of *n*-hexane into CH₂Cl₂ solution of the compound at 25 °C. The identity of **1–7** was confirmed by high-resolution MALDI FT-ICR (for **1** and **2**) or MALDI-TOF mass spectrometry (for **3–7**), which displayed the corresponding molecular ion (see the Supporting Information), and/or NMR spectroscopy, X-ray crystallography (for **1**), and elemental analysis. For acceptors **2**, **6**, and **7**, the NMR spectra could not be recorded due to the presence of paramagnetic species in the sample, as confirmed by electron paramagnetic resonance (EPR) spectroscopy (vide infra), and low solubility of the solid (¹H and ¹⁹F NMR spectra for **5** were obtained in one case, however, they could not be reproduced). Similar behavior has previously been described for other TCNQ-derived strong acceptors.^[6a,11]

Single crystals of **1** suitable for X-ray crystallographic analysis were obtained by slow diffusion of *n*-hexane into CH₂Cl₂ solution at 25 °C (Figure 1a). As already observed,^[13c] in the crystal packing of highly distorted **1**, two neighboring molecules undergo several dipolar CN⋯CN interactions (Figure 1b). The CN groups of one molecule interact with the C(CN)₂ moiety of its neighbor with the shortest

Table 1. Summary of the reactions of cyano-substituted alkynes **8–10** with TCNE, TCNQ, and F₄-TCNQ.

Cyanoalkyne	Acceptor	Product	Reaction conditions	Time	Yield [%]
	TCNE		[a]	4 days	97 ^[b]
	TCNQ		[c]	12 h	27 ^[b]
	F ₄ -TCNQ		[d]	17 h	65
	TCNE		[c]	16 h	26
	TCNQ		[c]	5 days	14
	F ₄ -TCNQ		[d]	16 h	84
	TCNE		[c]	2 days	66
	TCNQ		[f]	[f]	n.d.
	F ₄ -TCNQ		[d]	5 days	88

[a] In THF, 20 °C. [b] See reference [17]. [c] In 1,1,2,2-tetrachloroethane, 120 °C. [d] In CH₂Cl₂, 25 °C. [e] In 1,2-dichloroethane, 60 °C. [f] Under various reaction conditions, only traces of **4** were formed (MALDI-TOF MS).

contact of 3.02 Å observed between N16' and the central vinylic carbon atom C4. Consequently, two nearly orthogonal intermolecular CN...CN contacts between N16' and C7 or

atoms in **6**, an additional red shift of both CT bands to $\lambda_{\max} = 697$ nm (1.78 eV; $\epsilon = 40600$ M⁻¹ cm⁻¹) and $\lambda_{\max} = 942$ nm (1.32 eV; $\epsilon = 17000$ M⁻¹ cm⁻¹) occurs (Figure 2). Increasing

C5 of 3.17 and 3.12 Å, respectively, are formed. Similarly to DMA-substituted 1,1,4,4-tetracyanobuta-1,3-dienes (TCBDs)^[13b,c] and TCNQ adducts,^[15a] the DMA ring in **1** exhibits significant bond alternation, as expressed by its quinoid character (δr ; for its definition^[22] and bond lengths, see caption to Figure 1) of 0.052, indicative of efficient intramolecular CT interactions in the ground state.

The thermal stability of selected acceptors, that is essential for potential practical applications, was investigated by thermogravimetric analysis (TGA). The first observable decomposition temperatures, as determined by derivative thermogravimetry, ranged from 176 (for **7**) to 482 °C (for **2**) and presumably correspond to the loss of co-crystallized solvents. These decompositions are followed by a gradual weight loss in most cases (see the Supporting Information).

UV/Vis spectroscopy: Most of the DMA-substituted acceptors show in CH₂Cl₂ intense CT bands with end-absorptions reaching into the near infrared region (Figure 2). The UV/Vis absorption spectrum of hexacyano derivative **1** features the lowest-energy intramolecular CT band at 486 nm (2.55 eV; $\epsilon = 43300$ M⁻¹ cm⁻¹). Introduction of the cyclohexa-2,5-diene-1,4-diylidene spacer in **3** shifts the CT band to 633 nm (1.96 eV; $\epsilon = 13900$ M⁻¹ cm⁻¹), with a second, weaker CT band of lower energy appearing at $\lambda_{\max} = 930$ nm (1.33 eV; $\epsilon = 1400$ M⁻¹ cm⁻¹). Upon substitution of the TCNQ-derived moiety with the strongly electron-withdrawing fluorine

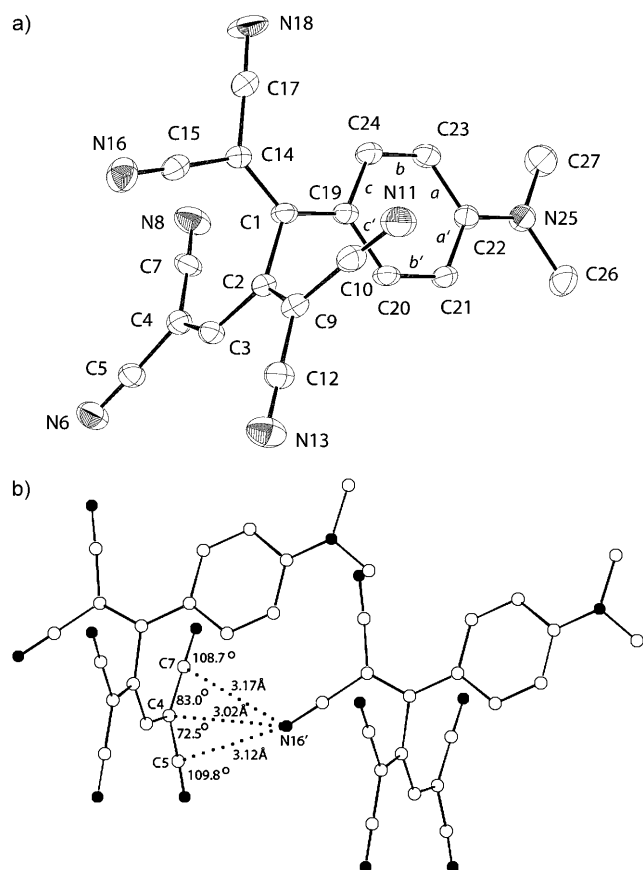


Figure 1. a) Molecular structure of **1** (ORTEP plot), arbitrary numbering, hydrogen atoms are omitted for clarity. Atomic displacement parameters obtained at 220 K are drawn at the 30% probability level. Selected bond lengths [Å] and bond angles [°]: C1–C2 1.516(5), C2–C3 1.448(5), C3–C4 1.366(5), C4–C5 1.433(5), C4–C7 1.412(6), C5–N6 1.140(5), C7–N8 1.146(5), C1–C14 1.376(5), C14–C17 1.442(5), C14–C15 1.427(6), C15–N16 1.153(5), C17–N18 1.134(5), C2–C9 1.358(5), C9–C12 1.429(6), C12–N13 1.139(5), C1–C19 1.417(5), C9–C10 1.442(6), C10–N11 1.141(5), C19–C20 1.415(5), C20–C21 1.363(5), C21–C22 1.405(5), C22–C23 1.413(5), C23–C24 1.362(5), C19–C24 1.423(5), C22–N25 1.354(5), N25–C27 1.460(5), N25–C26 1.470(5); C14–C1–C2 113.3(3), C15–C14–C17 112.9(3), C7–C4–C5 116.1(3), C12–C9–C10 115.7(3). Selected torsion angles [°]: C14–C1–C19–C24 –2.9(6), C14–C1–C2–C9 –93.2(4), C26–N25–C22–C21 –0.3(6). Quinoid character: $\delta r = (((a+a')/2 - (b+b')/2) + ((c+c')/2 - (b+b')/2))/2$.^[22] $\delta r = 0.052$. b) Arrangement of neighboring molecules in the crystal packing of **1**.

the number of the accepting CN groups, for example when going from fluorinated **5** to **7**, further lowers the energy of the CT bands. Indeed, absorption maxima at 753 nm (1.65 eV) and 1120 nm (1.11 eV), with an end-absorption near 1600 nm (0.78 eV), are observed for **7**. This low optical gap is quite remarkable for a small chromophore such as **7**.^[23] Protonation of the DMA moiety in **7** with trifluoroacetic acid (TFA) in CH₂Cl₂ eliminated these long-wavelength bands, whereas neutralization with K₂CO₃ regenerated partially (due to decomposition) the original spectrum, thus indicating the CT character of these bands (see the Supporting Information).

Electronic absorption spectra of **1–3**, **5**, **11**, and **12** were calculated by applying the spectroscopy oriented configura-

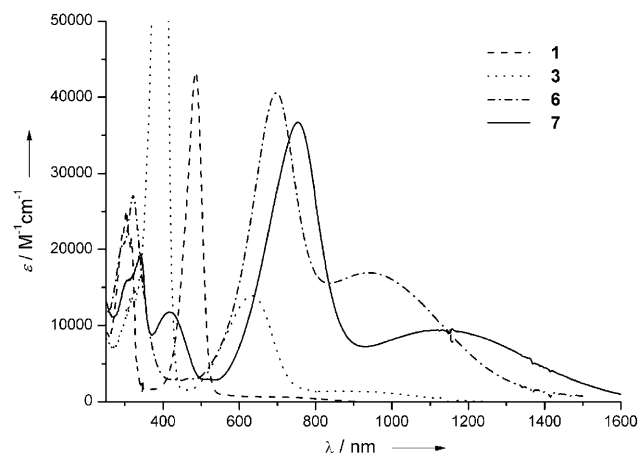


Figure 2. UV/Vis absorption spectra of acceptors **1**, **3**, **6**, and **7** in CH₂Cl₂ at 298 K. The high-intensity band of **3** at $\lambda_{\text{max}} = 400$ nm ($\epsilon = 108400 \text{ M}^{-1} \text{ cm}^{-1}$) is cut to allow enlargement of the weaker CT transitions.

tion interaction (SORCI)^[24] procedure implemented in the ORCA program suite.^[25] For acceptors **1–3** and **11**, the SORCI excitation energies are in good agreement with the experimental UV/Vis spectra recorded in CH₂Cl₂ (Table 2). However, the computational analysis for **5** and **12** did not reproduce the experimental values well (see the Supporting Information). According to theoretical data for **1–3** and **11**, the lowest energy excitation with high extinction coefficient (ϵ) and calculated high oscillator strength (f) can be assigned as a transition from the DMA-located HOMO to the LUMO+1 level located predominantly on the CN-containing acceptor moieties (for calculated HOMOs and LUMOs, see the Supporting Information). The oscillator strength of the HOMO→LUMO transition is rather small which is in agreement with weak or no extinction observed experimentally. The red shift of 1.22 eV of the longest-wavelength CT band observed in the UV/Vis spectra upon introduction of the cyclohexa-2,5-diene-1,4-diylidene spacer when moving from **1** (486 nm (2.55 eV)) to **3** (930 nm (1.33 eV)) is nicely reproduced in the SORCI spectra and amounts to 1.54 eV, with the deviation from the experimental value being within the usual error range of the method.

Whereas the optimized geometries of acceptors of **1–3** and **11** show almost perpendicular CN-containing moieties with respect to the DMA ring, and the cyclohexa-2,5-diene-1,4-diylidene spacer in **3**, it is not the case for **5** and **12** (see the Supporting Information). Consequently, the LUMO and LUMO+1 are no longer localized on either the central C atom connecting the DMA ring with the CN-containing moieties (LUMO+1) or the CN-acceptor itself (LUMO), which results in a more difficult configuration interaction problem and less accurate SORCI spectra (unless this problem is explicitly taken care of in the choice of the reference space). Thus, the first excited state with high oscillator strength for **5** and **12** is assigned to a mixture of a HOMO→LUMO+1 single excitation and an excitation of both electrons of the HOMO to the LUMO. The

Table 2. Experimental electronic transitions for **1–3** and **11**, derived from the UV/Vis spectra in CH₂Cl₂, and computed SORCI excitation spectra.

	Experimental		Computed values ^[a]		Composition of band	CI coefficients ^[b]
	λ [nm (eV)]	ϵ [M ⁻¹ cm ⁻¹]	λ [nm (eV)]	f		
1	486 (2.55)	43 300	454 (2.73)	0.81	H→L+1	0.94
	317 (3.91)	21 400				
	304 (4.08)	2500	303 (4.09)	0.92	H→L H→L+1	0.37 0.59
2	657 (1.89)	5600	676 (1.83)	0.12	H→L	0.92
	469 (2.65)	16 300	466 (2.66)	0.33	H→L+1	0.89
			364 (3.41)	0.20	H→L+1	0.75
	295 (4.21)	15 400	311 (3.99)	0.25	H→L+1 H→L+1	0.54 0.31
3	930 (1.33)	1400	1045 (1.19)	0.10	H→L	0.88
			639 (1.94)	0.80	H→L+1	0.88
	633 (1.69)	13 900	632 (1.96)	0.16	H→L+1	0.79
	400 (3.10)	10 8400	414 (3.00)	0.13	H→L+1	0.81
11 ^[c]	643 (1.93)	3200	545 (2.27)	0.21	H→L	0.95
	450 (2.76)	30 000	418 (2.96)	0.51	H→L+1	0.88

[a] Only excitations with oscillator strength larger than 0.10 are shown for the calculated spectra; f =oscillator strength; H=HOMO; L=LUMO; CI=configuration interaction. [b] Correspond to the final state. [c] Taken from ref. [17].

HOMO→LUMO+1 excitation of compounds **5** and **12** is calculated at higher energies.

Electrochemistry: The redox properties of acceptors **1–3**, **5–7**, and the reference compounds TCNE, TCNQ,^[26] and F₄-TCNQ were investigated by cyclic voltammetry (CV) and rotating-disc voltammetry (RDV) in CH₂Cl₂ (+0.1 M *n*Bu₄NPF₆, all potentials vs. the ferricinium/ferrocene couple (Fc⁺/Fc)) and are summarized in Table 3. The DMA donor moiety in all studied acceptors undergoes a one-electron oxidation step that is irreversible (CV), except for **1**, **6**, and previously reported **11**, and **13**. An anodic shift of 140 mV is observed for the oxidation step upon introduction of the additional CN group into the buta-1,3-diene-1,4-diyl moiety when going from DMA-substituted 1,1,4,4-tetracyanobuta-1,3-diene (TCBD) derivative **13** ($E_{\text{ox},1} = +0.86$ V),^[13c] to PCBD **11** (+1.00).^[17] In contrast, the effect of substitution with stronger DCV (–CH=C(CN)₂) (in **1**) or TCV (–C(CN)=C(CN)₂) (in **2**) acceptor moieties is much less pronounced and TCNE adducts **1** and **2** are oxidized at lower potentials of +0.97 and +0.91 V, respectively. The extra CN group in cyclohexa-2,5-diene-1,4-diylidene-expanded PCBD **12** (+0.52 V) shifted its oxidation step anodically by 100 mV, compared to TCNQ adduct **14**, which is irreversibly oxidized at +0.42 V. Again, DCV-substituted **3** undergoes its oxidation step at +0.50 V, which corresponds to a shift of only 80 mV compared to **14**. An anodic shift of 90 mV is observed for the oxidation step upon F-substitution of the TCNQ moiety in **5** (+0.61 V) and **6** (+0.59 V) compared to their TCNQ counterparts **12** and **3**, respectively. Overall, the oxidations of TCNQ adducts **3**, **12**, and **14** (or fluorinated **5–7**) are occurring at significantly lower potentials compared to the TCNE adducts **1**, **2**, and **13**, which indicates less efficient ground state CT interactions between the DMA donor moiety and the CN accepting groups in these chromophores (vide infra).

More importantly, the studied compounds undergo two (**5**) or three (**1–3**, **6**, and **7**) reversible one-electron reduction steps centered on the CN-containing moieties, eventually followed by the fourth irreversible electron transfer for fluorinated **6** and **7**. We have previously found that the additional CN group in PCBD **11** ($E_{\text{red},1} = -0.30$ V)^[17] facilitated the first reduction step by 390 mV when compared to TCBD **13**, which is reversibly reduced at –0.69 V.^[13c,27] As expected, the incorporation of stronger acceptor moieties in DCV-substituted **1** and TCV-substituted **2** further shifts the observed reduction steps towards more

positive potentials. Thus, the introduction of the additional DCV moiety upon moving from TCBD **13** to TCNE adduct **1** (–0.22 V) shifts the first reduction step anodically by 470 mV to occur at more positive potential than that of TCNE (–0.32 V) or TCNQ (–0.25 V). Although only poorly resolved CV traces were obtained for TCV-substituted TCNE adduct **2**, the first reversible electron uptake occurs at +0.12 V, which represents an unprecedented anodic shift of 810 mV with respect to parent **13**. On the other hand, only less pronounced effects are observed between TCNQ-derivative **14** (–0.50 V)^[15a] and expanded PCBD **12** reduced at –0.27 V^[17] or DCV-substituted **3** (–0.28 V).

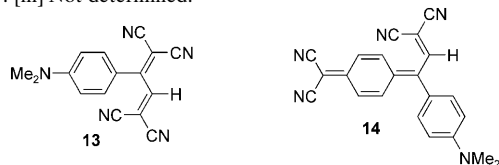
Noticeable for the new chromophores **1–3** and **5–7** is the facility of the second one-electron reduction step ($E_{\text{red},2}$ between –0.92 (for **1**) and –0.17 V (for **7**)) which is irreversible for chromophore **1**. In addition, unprecedented third reversible one-electron reduction steps are observed for **1–3**, **6**, and **7** ranging from –2.30 V (for **1**) to –1.19 V (for **7**).

As a result of F-substitution in derivatives **5–7**, the reversible reduction steps became notably facilitated with respect to their TCNQ analogues.^[28] Thus, the two reversible reduction steps of fluorinated cyclohexa-2,5-diene-1,4-diylidene-expanded PCBD derivative **5** occur anodically shifted by 270 and 260 mV at ±0.00 and –0.27 V, respectively, compared to TCNQ derivative **12** (–0.27 and –0.53 V).^[17] Furthermore, spectroelectrochemical studies of **5** performed in a optically transparent thin-layer electrode (OTTLE) suggest that the electrogenerated reduced species (i.e. radical anion and dianion) are persistent at the time scale of spectroelectrochemistry, namely at least for 60 s (see the Supporting Information). The three one-electron transfers of DCV-substituted **6** occurring at –0.10, –0.25, and –1.76 V appear shifted, compared to **3**, to more positive potentials by 180, 220, and 100 mV, respectively. The introduction of the additional CN group upon moving from **6** to **7** further

Table 3. Cyclic voltammetry (CV; scan rate $\nu=0.1 \text{ V s}^{-1}$) and rotating disk voltammetry (RDV) data of **1–3**, **5–7**, and **11–14**, and the reference compounds TCNE, TCNQ, and F_4 -TCNQ in CH_2Cl_2 (+0.1 M $n\text{Bu}_4\text{NPF}_6$).^[a] Calculated adiabatic electron affinity (EA), based on the BP86/def-TZVP COSMO($\epsilon=4.5$)/BP86/def-SV(P) method.

	CV			RDV		EA [eV]
	E° [V] ^[b]	ΔE_p [mV] ^[c]	E_p [V] ^[d]	$E_{1/2}$ [V] ^[e]	Slope [mV] ^[f]	
1	+0.97	90		+0.95 (1 e ⁻)		4.49
	-0.22	80		-0.26 (1 e ⁻)	60	
2	-2.30	120		-0.99 (1 e ⁻)	90	4.87
	+0.12 ^[h]	60	+0.91 ^[g]	+0.12 (1 e ⁻)	65	
3	-1.88	60				4.51
			+0.50	+0.47 (1 e ⁻)	80	
	-0.28	60		-0.32 (1 e ⁻)	65	
	-0.47	70		-0.54 (1 e ⁻)	65	
5	-1.86	60		-1.94 (1 e ⁻)	60	4.66
			+0.61 ^[g]			
	± 0.00	75		± 0.00 (1 e ⁻)	68	
6	-0.27	70		-0.29 (1 e ⁻)	61	4.69
	+0.59	80				
	-0.10	60		-0.11 (1 e ⁻)	55	
	-0.25	60		-0.26 (1 e ⁻)	55	
7 ^[i]	-1.76	70				4.98
			-2.26			
			+0.64	+0.16 (1 e ⁻)	60	
	+0.16	80		-0.19 (1 e ⁻)	60	
11 ^[j]	-0.17	60		-1.24 (1 e ⁻)		4.36
	-1.19	80		-1.99 (1 e ⁻)		
	+1.00	90	-1.94	+1.00 (1 e ⁻)	65	
12 ^[j]	-0.30	90		-0.30 (1 e ⁻)	65	4.42
	-0.85	100		-0.85 (1 e ⁻)	100	
13 ^[k]			+0.52	+0.54 (1 e ⁻)	50	[m]
	-0.27	80		-0.28 (1 e ⁻)	60	
	-0.53	85		-0.56 (1 e ⁻)	60	
	+0.86	80		+0.87 (1 e ⁻)	70	
14 ^[l]	-0.69	80		-0.70 (1 e ⁻)	70	[m]
	-1.26	90		-1.38 (1 e ⁻)	140	
	-0.50	80	+0.42	+0.44 (1 e ⁻)	60	
TCNE	-0.76	80		-0.55 (1 e ⁻)	70	4.57
	-0.32			-0.86 (1 e ⁻)	70	
TCNQ	-1.35					4.59
	-0.25	90		-0.26 (1 e ⁻)	75	
F_4 -TCNQ	-0.81	90		-0.87 (1 e ⁻)	75	4.96
			+1.11 ^[g]			
	+0.16	90		+0.19 (1 e ⁻)	75	
	-0.46	100		-0.48 (1 e ⁻)	85	

[a] All potentials are given versus the Fc^+/Fc couple used as internal standard. [b] $E^\circ = (E_{pc} + E_{pa})/2$, where E_{pc} and E_{pa} correspond to the cathodic and anodic peak potentials, respectively. [c] $\Delta E_p = E_{ox} - E_{red}$, where the subscripts ox and red refer to the conjugated oxidation and reduction steps, respectively. [d] E_p = Irreversible peak potential. [e] $E_{1/2}$ = Half-wave potential. [f] Slope = Slope of the linearized plot of E versus $\log[I/(I_{lim} - I)]$, where I_{lim} is the limiting current and I the current. [g] Electrode inhibition during oxidation. [h] Poorly resolved second reduction. [i] Contains a small amount of 7^- (see the Supporting Information). [j] Taken from ref. [17]. [k] Taken from ref. [13c]. [l] Taken from ref. [15a]. [m] Not determined.



shifts the first electron uptake to more positive potentials by 260 mV.^[27] While the first reduction potential for **7** is the same as that of F_4 -TCNQ (+0.16 V), the second is, similarly to our previous observations^[17] significantly facilitated (-0.17 (**7**) vs. -0.46 V (F_4 -TCNQ)) and is followed by two reversible one-electron transfers at -1.19 and -1.94 V. It has to be mentioned that a trace of one-electron reduced species (radical anion) has been detected by RDV in freshly prepared CH_2Cl_2 solutions of **7**, thus underscoring its exceptional electron-accepting power (see the Supporting Information).

An electron-withdrawing group involved in a donor-acceptor π -conjugated system generally hampers the oxidation, as it decreases the electron density on the oxidizable donor moieties, and conversely, an electron-donating group hinders the electron reduction by delivering electrons into the acceptor. In this respect, our findings might be rather surprising, as gradual shifts of both the oxidation and the reduction steps towards more positive potentials are expected upon increasing the electron-accepting power of the CN-containing substituents. Nevertheless, at the same time as the acceptor strength increases, as expressed by Hammett constants σ_p of +0.66 (-CN), +0.84 (-CH=C(CN)₂), and +0.98 (-C(CN)=C(CN)₂),^[29] the substituents become sterically more demanding. This consequently, together with electrostatic repulsion between the negatively polarized N-atoms in neighboring CN groups, renders the whole molecule highly twisted (as revealed by X-ray crystallography and theoretical calculations). Under these conditions, efficient π -conjugation between the donor and acceptor moieties becomes impaired to a certain extent, as already previously observed,^[13c] which makes any straightforward correlation between the observed redox potentials and the acceptor strength rather difficult.

The optical HOMO-LUMO gaps, determined from the end-absorption λ_{end} of the longest-wavelength UV/Vis band, correlate reasonably well ($R^2 = 0.895$) with the electrochemical gaps $\Delta(E_{ox,1} - E_{red,1})$ suggesting that the same orbitals are involved in both optical and electrochemical gaps for **1–3**, **5–7**, and **11–14** (Table 4 and Figure 3). Furthermore, the

Table 4. Optical and electrochemical gaps of TCNE, TCNQ, and F_4 -TCNQ adducts **1–3**, **5–7**, and **11–14** determined from UV/Vis spectroscopy and CV in CH_2Cl_2 .

	λ_{max} [nm (eV)]	λ_{end} [nm (eV)]	$\Delta(E_{ox,1} - E_{red,1})$ [V]
1	486 (2.55)	920 (1.35)	1.19
2	657 (1.89)	1100 (1.13)	0.79
3	930 (1.33)	1270 (0.98)	0.78
5	993 (1.25)	1500 (0.83)	0.61
6	942 (1.32)	1400 (0.89)	0.69
7	1120 (1.11)	1640 (0.76)	0.48
11 ^[a]	643 (1.93)	820 (1.51)	1.30
12 ^[a]	859 (1.44)	1300 (0.95)	0.79
13 ^[b]	570 (2.18)	860 (1.44)	1.55
14 ^[c]	759 (1.63)	1050 (1.18)	0.99

[a] Taken from ref. [17]. [b] Taken from ref. [13c]. The originally reported λ_{end} of 960 nm (1.29 eV) was apparently overestimated. [c] Taken from ref. [15a].

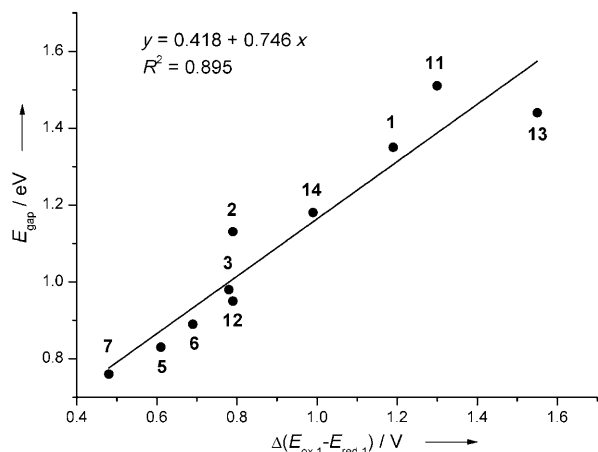


Figure 3. Linear correlation between the optical gap E_{gap} , determined from λ_{cnd} , and electrochemical gap $\Delta(E_{\text{ox},1} - E_{\text{red},1})$ for acceptors **1–3**, **5–7**, and **11–14**.

electrochemical gap decreases in the sequence **13** > **11** > **1** > **2** reflecting the increased acceptor strength of the CN-containing substituents as mentioned above.

The electron-accepting power, expressed as adiabatic electron affinity (EA), has been calculated (BP86/def-TZVP COSMO($\epsilon=4.5$)/BP86/def-SV(P))^[30] for acceptors **1–7**, **11** and **12** as well as for the reference compound F₄-TCNQ (Table 3).^[31] A good linear correlation ($R^2=0.857$) exists between the calculated EAs and the first reduction potentials $E_{\text{red},1}$ (Figure 4). Despite the substitution with strong DMA

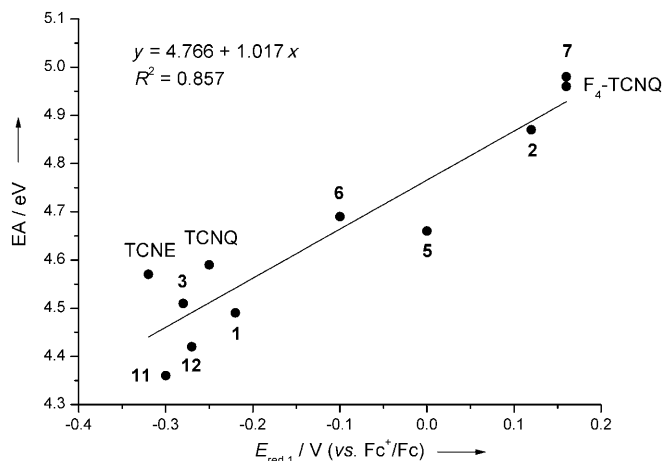


Figure 4. Linear correlation between the calculated adiabatic electron affinity EA (BP86/def-TZVP COSMO($\epsilon=4.5$)/BP86/def-SV(P)) for **1–3**, **5–7**, **11**, and **12**, F₄-TCNQ, TCNQ, and TCNE against $E_{\text{red},1}$ determined by CV.

donors, the predicted EAs for **2** (4.87 eV) and **7** (4.98 eV) rival the value calculated for the state-of-the-art p-type dopant F₄-TCNQ (4.96 eV),^[10] which makes them interesting for potential applications in optoelectronic devices.

Initial EPR investigations: Due to difficulties encountered during attempted NMR characterization (vide supra), the samples of acceptors **2** and **5–7** were investigated by means of EPR spectroscopy. Indeed, paramagnetic character of the samples both in the solid state and solution was found in all cases. EPR spectra of remarkable intensity were obtained for solid samples of **2** and **5–7** at ambient temperature. Dissolving **2**, **6**, and **7** in [D₆]acetone and **5** in 1,2-dimethoxyethane (DME) again led to intense EPR spectra both in liquid and frozen solution (for EPR spectra of **2** and **7**, see Figure 5; for **6**, see the Supporting Information). The obtained spectra are unresolved in all cases, whereas broader lines are observed due to anisotropic interactions in the solid state. Nevertheless, the virtually matching *g* factors indicate that the EPR signals observed for **2** and **5–7** in the solid-state and solution result from compatible electronic structures (Table 5).

Furthermore, reduction of **5** with K metal in DME at 270 K yielded an intense EPR spectrum that is compatible in terms of its shape and *g* factor to that of **5** recorded both in the solid state and DME solution (see the Supporting Information). The data is in good agreement with the published values for radical anions of TCNE, TCNQ, and F₄-TCNQ.^[32] Owing to the very low first reduction potentials of **2**, and **5–7**, it can be anticipated that the corresponding radical anions are at least partly present under the applied experimental conditions, as observed by others.^[6a,11]

Charge-transfer salt {[FeCp*₂]⁺]₂[12]₂²⁻ (15**):** While exploring the ability of the TCNQ-derived acceptor **12** to form charge-transfer complexes with various electron donors, we found that the TCNQ moiety in **12** undergoes reductive σ -dimerization upon reaction with the strong electron donor decamethylferrocene ([FeCp*₂]⁺; $E_{\text{ox},1} = -0.59$ V),^[20] as previously observed for TCNQ.^[33]

Thus, an intense green solution was obtained upon addition of yellow [FeCp*₂] in CH₂Cl₂ to the originally deep-purple solution of **12** in dry acetonitrile at 25 °C. The solid obtained after evaporation of the solvents was recrystallized by slow diffusion of *n*-hexane into CH₂Cl₂ solution to afford dark-green crystals of {[FeCp*₂]⁺]₂[12]₂²⁻ (**15**) in 68% yield. The obtained crystals of **15** incorporated, even after prolonged drying in vacuo, remaining co-crystallized CH₂Cl₂ molecules, as indicated by elemental analysis and TGA that are in good agreement with the formula {[FeCp*₂]⁺]₂[12]₂²⁻·1.4 CH₂Cl₂ (see the Supporting Information).

The X-ray crystal structure of **15** consists of two independent [12]₂²⁻ ions (designated as molecule **A** and **B**), four [FeCp*₂]⁺ molecules, one of which is disordered, and three disordered CH₂Cl₂ molecules (Figure 6, for details, see the Experimental Section; for molecule **B**, see the Supporting Information).^[34] The two dimeric ions [12]₂²⁻ feature long central C–C bonds (C105–C106 and C156–C157) of 1.63 Å which are comparable to those in reported (TCNQ)₂²⁻ σ -dimers.^[33] Consequently, the involved C-atoms are practically tetrahedral with the bond angles ranging from 105.3° (C135–C105–C106) to 113.0° (C102–C105–C106). The uni-

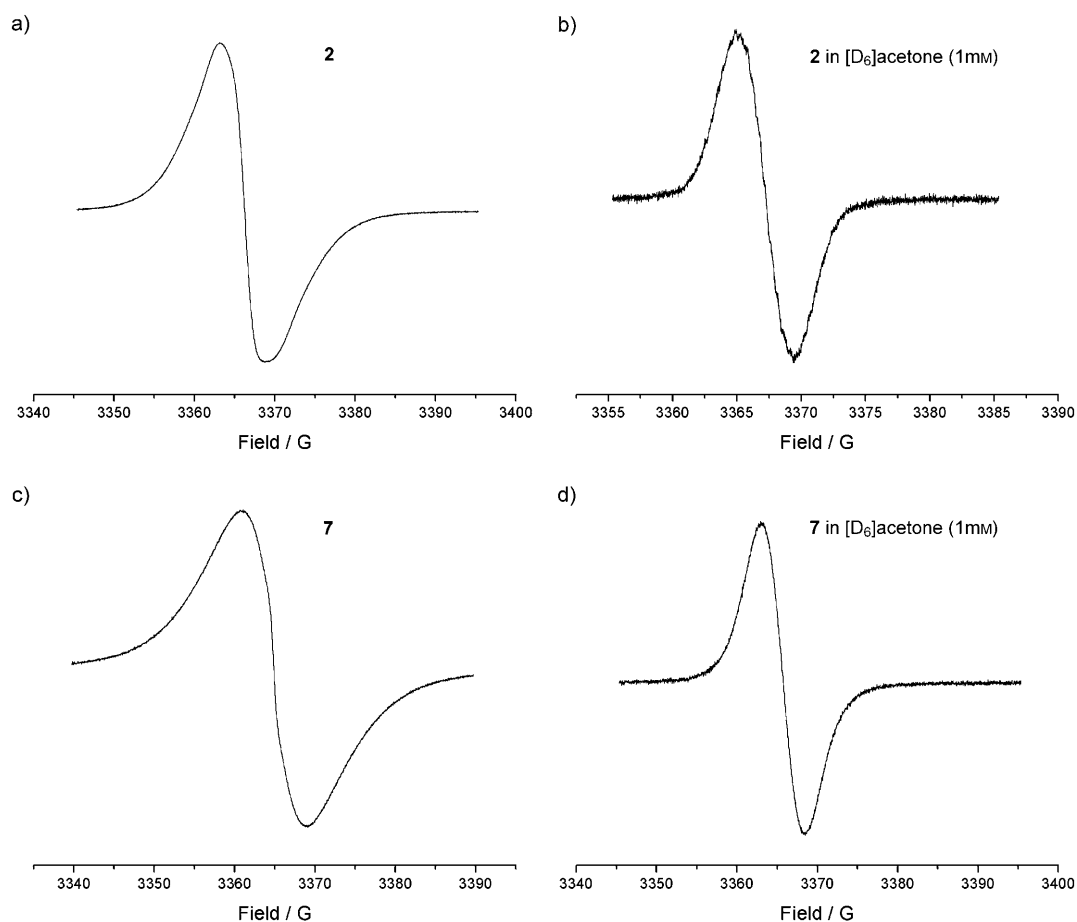


Figure 5. EPR spectra of **2** and **7** in the solid state (a and c) and in $[D_6]$ acetone solution (b and d) recorded at ambient temperature (ca. 298 K).

Table 5. The g factors extracted from the EPR spectra of **2**, **5**, and **7**, recorded under various conditions, and the g factors for the reference compounds TCNE, TCNQ, and F_4 -TCNQ.

Compound	Conditions	g factor
2	solid state	2.0036
	$[D_6]$ acetone solution (1 mm)	2.0034
5	solid state	2.0032
	DME solution (270 K)	2.0034
	after K metal reduction in DME (270 K)	2.0035
7	solid state	2.0033
	$[D_6]$ acetone solution (1 mm)	2.0032
TCNE $^{2-}$	^[a]	2.0026 ± 0.0002
TCNQ $^{2-}$	^[b]	2.0027 ± 0.0002
F_4 -TCNQ $^{2-}$	^[b]	2.0029 ± 0.0001

[a] Taken from ref. [32a]. [b] Taken from ref. [32b].

formity of the distances in the originally quinoid TCNQ rings in $[12]_2^{2-}$, averaging to 1.39 Å for both independent molecules, suggests that their aromatization occurred upon σ -dimer formation. Furthermore, the significant lengthening of the C=C bonds in the TCV ($-C(CN)=C(CN)_2$) moieties to an average value of 1.44 Å with the concurrent shortening of the adjacent C–C bonds to 1.37 Å indicate delocalization of the negative charge over the entire TCV unit, hence forming tricyano-substituted allylic anions (Figure 6 a). Simi-

lar effects have previously been described for other anionic TCV-substituted systems.^[35] This is further supported by calculations at the B3LYP/6-31G(d) level^[36] performed on the $[12]_2^{2-}$ σ -dimer. The bond lengths and torsional angles of the calculated dianionic structure compare well to those obtained by X-ray analysis (see caption to Figure 6 a). The calculated HOMO of the dianionic species has most of the electron density on the TCV moieties with only small coefficients on the central C–C bond (see the Supporting Information).

In the crystal packing of **15**, multiple short contacts with $N \cdots C$ distances ranging from 3.35 to 3.58 Å between the $[12]_2^{2-}$ ions (**A** and **B**) and the neighboring $[FeCp^*_2]^+$ molecules are observed. For example, molecule **A** is surrounded by eight $[FeCp^*_2]^+$ units with ten intermolecular $N \cdots C$ contacts between 3.36 and 3.61 Å (Figure 6 b; for molecule **B**, see the Supporting Information). The average Fe–C bond lengths of 2.097 Å, based on the three ordered $[FeCp^*_2]^+$ units, are consistent with the presence of Fe^{III} atoms.^[37]

Naturally, the σ -bond formation between two radical centers results in disappearance of paramagnetic properties. In analogy to the reported TCNQ σ -dimers, the central C–C bond in diamagnetic $[12]_2^{2-}$ is expected to be rather weak due to the long bond length, considerable delocalization of

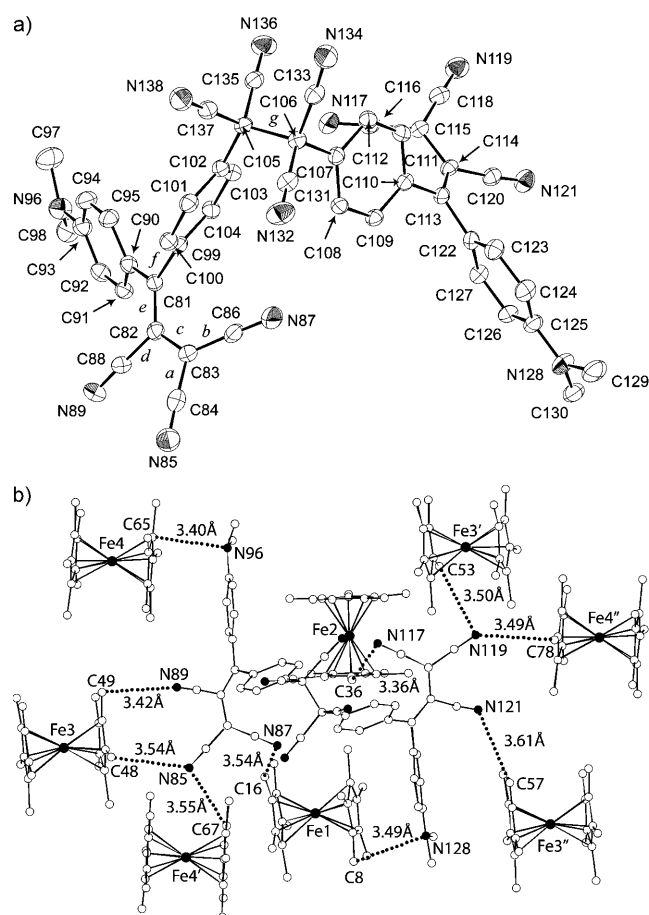
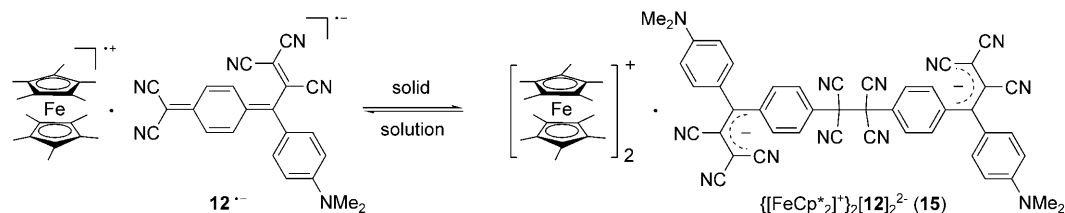


Figure 6. a) ORTEP plot of dianion $[12]_2^{2-}$ (molecule **A**) in the X-ray crystal structure of **15**. Atomic displacement parameters obtained at 220 K are drawn at the 30% probability level. Hydrogen atoms and CH_2Cl_2 molecules are omitted for clarity. Selected experimental^[34] and calculated (in parentheses; B3LYP/6-31G(d))^[36] bond lengths [Å]: *a* 1.41 (1.41), *b* 1.41 (1.42), *c* 1.44 (1.45), *d* 1.45 (1.45), *e* 1.37 (1.39), *f* 1.48 (1.48), *g* 1.63 (1.67). Selected experimental^[34] and calculated (in parentheses; B3LYP/6-31G(d))^[36] torsion angles [°]: C81-C82-C83-C84 162.7 (163.5), C99-C81-C82-C83 167.7 (161.2), C82-C81-C90-C95 140.6 (137.8), C82-C81-C99-C104 135.2 (141.0). b) Arrangement of neighboring molecules in the crystal packing of **15** showing ten intermolecular N...C contacts between $[12]_2^{2-}$ (molecule **A**) and the eight surrounding $[\text{FeCp}^*]_2^+$ molecules. The shortest contact between two neighboring molecules of type **A** (N117–C129 3.16 Å) is not shown.

the bonding electrons, and electrostatic repulsions.^[33c,38] Breaking this bond by external stimuli should yield two radical anions $12^{\cdot-}$ (Scheme 1). Indeed, the solid-state IR spectrum of **15** displays two bands in the $\nu(\text{C}\equiv\text{N})$ region at 2169



Scheme 1. Formation and dissociation of dimeric $\{[\text{FeCp}^*]_2^+\}_2[12]_2^{2-}$ (**15**).

and 2129 cm^{-1} , accompanied by a band at 806 cm^{-1} resulting from the $\delta(\text{C-H})$ bend, which are attributable to the σ -bonded TCNQ moieties.^[39] The IR spectrum recorded in CHCl_3 solution of **15** on the other hand features a single band at $\nu(\text{C}\equiv\text{N})=2178\text{ cm}^{-1}$ and a weak band at 839 cm^{-1} , which most likely results from the $\delta(\text{C-H})$ mode (see the Supporting Information), thus indicating dissociation of the central σ -bond to form two radical anions $12^{\cdot-}$ in solution. Moreover, the solid obtained upon evaporation of the CHCl_3 solution gave identical IR spectrum to that of pristine **15**. This is further supported by preliminary EPR investigations both in the solid state and solution. Whereas the solid sample of **15** containing diamagnetic σ -dimers $[12]_2^{2-}$ is EPR silent both at 290 and 180 K, dissolving **15** in DME results in appearance of intense EPR spectra apparently resulting from radical anion $12^{\cdot-}$ (see the Supporting Information). This is in agreement with the fact that no NMR spectra of **15** could be obtained in CD_2Cl_2 or $[\text{D}_6]$ acetone solution.

The influence of the counter cation, solvent polarity, concentration, and temperature on the σ -dimerization process is currently under investigation.^[38]

Conclusions

A series of stable organic super-acceptors has been synthesized by thermal [2+2] cycloadditions of TCNE, TCNQ, and F_4 -TCNQ to DMA-substituted alkynes bearing either nitrile, dicyanovinyl, or tricyanovinyl functions, followed by retro-electrocyclization of the initially formed cyclobutenes. Despite the nonplanarity of these acceptors, as revealed by X-ray crystallographic analysis (for **1**) and theoretical calculations, efficient intramolecular charge-transfer (CT) interactions are established. The corresponding CT bands appear strongly bathochromically shifted with an end-absorption reaching far into the near infrared region, down to 1600 nm (0.78 eV) for F_4 -TCNQ adduct **7**. Electronic absorption spectra of **1–3**, **5**, **11**, and **12** were calculated by applying the spectroscopy oriented configuration interaction (SORCI) procedure. In most cases the SORCI excitation energies are in good agreement with the experimental UV/Vis spectra recorded in CH_2Cl_2 . The electrochemical investigations of these acceptors by CV and RDV in CH_2Cl_2 identified their remarkable propensity for reversible electron uptake rivaling in some cases even the benchmark compound F_4 -TCNQ ($E_{\text{red},1}=+0.16\text{ V vs. Fc}^+/\text{Fc}$). Furthermore, the electron-

accepting power of the new compounds expressed as adiabatic electron affinity has been estimated by theoretical calculations. Despite the substitution with strong DMA donors, the predicted EAs for acceptors **2** and **7** reach the value calculated for F₄-TCNQ (4.96 eV), which makes these compounds interesting for potential applications as p-type dopants in the fabrication of OLEDs or solar cells.

The first example of a charge-transfer salt between the DMA-substituted TCNQ adduct **12** and strong electron donor decamethylferrocene has been prepared. The X-ray crystallographic analysis revealed that the TCNQ moiety in the acceptor underwent reductive σ -dimerization upon reaction with the donor. Initial investigations by EPR and IR spectroscopy both in the solid state and solution suggest, that the dimeric species dissociates in solution. Detailed investigations of this phenomenon as well as attempts to prepare conductive or magnetic charge-transfer salts between these potent acceptors and various organic and organometallic donors are currently being pursued. We believe that even stronger acceptors are in reach upon careful choice of reacting partners in the [2+2] cycloadditions.

Experimental Section

Materials and general methods: Reagents and solvents were purchased at reagent grade from Acros, Aldrich, and Fluka, and used as received. CH₂Cl₂ was freshly distilled from CaH₂ under N₂. All reactions were performed under an inert atmosphere by applying a positive pressure of N₂. Column chromatography (CC) and plug filtrations were carried out with SiO₂ 60 (particle size 0.040–0.063 mm, 230–400 mesh ASTM; Fluka) or SiO₂ 60 (particle size 0.063–0.200 mm, 70–230 mesh ASTM; Merck) and distilled technical solvents. 3-[4-(Dimethylamino)phenyl]-2-propynenitrile (**8**),^[17,18] 3-[4-(dimethylamino)phenyl]-2-propyn-1-ylidene]propanedinitrile (**9**),^[13b] 4-[4-(dimethylamino)phenyl]-1-buten-3-yn-1,1,2-tricarbonitrile (**10**),^[19] and 3-(dicyanomethylidene)-2-[4-(dimethylamino)phenyl]-1,4-pentadiene-1,1,5,5-tetracarbonitrile (**12**),^[17] were prepared according to literature procedures. Thin-layer chromatography (TLC) was conducted on aluminum sheets coated with SiO₂ 60 F₂₅₄ obtained from Macherey–Nagel; visualization with a UV lamp (254 or 366 nm). Melting points (m.p.) were measured on a Büchi B-540 melting-point apparatus in open capillaries and are uncorrected. ¹H NMR, ¹³C NMR, and ¹⁹F NMR spectra were measured on a Varian Gemini 300 or on a Bruker DRX400 or on a Bruker DRX500 spectrometer at 298 K. Chemical shifts (δ) are reported in ppm relative to the signal of tetramethylsilane (TMS). Residual solvent signals in the ¹H and ¹³C NMR spectra were used as an internal reference. Coupling constants (*J*) are given in Hz. The apparent resonance multiplicity is described as s (singlet), br s (broad singlet), d (doublet), t (triplet), q (quartet), and m (multiplet). Infrared spectra (IR) were recorded on a Perkin–Elmer BX FT-IR spectrometer; signal designations: s (strong), m (medium), w (weak). UV/Vis spectra were recorded on a Varian Cary-5 spectrophotometer. The spectra were measured in CH₂Cl₂ in a quartz cuvette (1 cm) at 298 K. The absorption maxima (λ_{max}) are reported in nm with the extinction coefficient (ϵ) m⁻¹cm⁻¹ in brackets; shoulders are indicated as sh. High-resolution (HR) EI-MS spectra were measured on a Micromass AutoSpec-Ultima spectrometer. HR FT-ICR-MALDI spectra were measured on an IonSpec Ultima Fourier transform (FT) instrument with [(2E)-3-(4-*tert*-butylphenyl)-2-methylprop-2-enylidene]malononitrile (DCTB) or 3-hydroxypicolinic acid (3-HPA) as matrix. HR MALDI-TOF spectra were recorded on a Bruker Ultraflex II mass spectrometer using 7,7,8,8-tetracyanoquinodimethane (TCNQ) as matrix and internal calibration (Bruker High Precision Calibration Mode) with TCNQ ([M]⁺, C₁₂H₄N₄⁺, *m/z* calc. 204.0430; Fluka), terthiophene ([M]⁺, C₁₂H₈S₃⁺, *m/z* calcd 247.9783; Fluka), and hexahy-

dro-2,6-bis(2,2,6,6-tetramethyl-4-piperidinyl)-1,4,5,8,8H-2,3a,4a,6,7a,8a-hexaazacyclopenta[def]fluor-ene-4,8-dione ([M+H]⁺, C₂₆H₄₆N₈O₂⁺, *m/z* calcd 503.3816; Uvinul 4049 H Ciba Speciality Chemicals). The most important peaks are reported in *m/z* units with *M* as the molecular ion. Thermogravimetric analyses (TGA) were carried out on a TA Instruments TGA Q500 V5.3 instrument in air, at a heating rate of 20°Cmin⁻¹ between 50°C and 900°C. Elemental analyses were performed by the Mikrolabor at the Laboratorium für Organische Chemie, ETH Zürich, with a LECO CHN/900 instrument, fluorine was estimated by ionchromatography on a Metrohm 761 Compact IC instrument, chlorine was estimated by argentometric titration.

Electrochemistry: The electrochemical measurements were carried out at 20°C in CH₂Cl₂, containing 0.1 M *n*Bu₄NPF₆ in a classical three-electrode cell. CH₂Cl₂ was purchased in spectroscopic grade from Merck, dried over molecular sieves (4 Å), and stored under Ar prior to use. *n*Bu₄NPF₆ was purchased in electrochemical grade from Fluka and used as received. The working electrode was a glassy carbon disk electrode (3 mm in diameter) used either motionless for cyclic voltammetry (0.1 to 10 V s⁻¹) or as rotating-disk electrode for rotating disk voltammetry (RDV). The auxiliary electrode was a Pt wire, and the reference electrode was either an aqueous Ag/AgCl electrode or a platinum wire used as a pseudo-reference electrode. All potentials are referenced to the ferricinium/ferrocene (Fc⁺/Fc) couple, used as an internal standard, and are uncorrected from ohmic drop. The cell was connected to Autolab PGSTAT30 potentiostat (Eco Chemie BV, Utrecht, The Netherlands) controlled by the GPSE software running on a personal computer.

EPR measurements: EPR spectra were recorded on a Bruker ESP 300 X-band spectrometer. All measurements were performed at ambient temperature (ca. 298 K), unless otherwise stated. 1,2-Dimethoxyethane (DME) was heated to reflux over Na/K alloy and stored over Na/K alloy under high vacuum. [D₆]acetone was used as received. Compounds **2**, **6**, and **7** were dissolved in [D₆]acetone and deoxygenated thoroughly by argon bubbling through for 10 min. Reduction of **5** was performed by contact of the DME solution of the parent compound with a K-metal mirror under high vacuum.

Calculations: Electronic absorption spectra of **1–3**, **5**, **11**, and **12** were calculated by applying the spectroscopy oriented configuration interaction (SORCI)^[24] procedure implemented in the ORCA program suite.^[25] The geometries of all molecules were optimized by using the TURBOMOLE program suite, version 5.10^[40] at the BP86/def-SV(P) level. A single-point Hartree–Fock calculation using the TZVP basis set^[41] was performed to generate the input for the SORCI calculation. The active space was constructed from all Slater determinants distributing altogether six electrons in the HOMO–2, HOMO–1, HOMO, LUMO, and LUMO+1 of the Hartree–Fock calculation, preserving the HF-occupation of all other orbitals. The three configuration selection parameters were set to 10⁻⁶ (tsel), 10⁻⁴ (tpre), and 10⁻⁵ (tnat), respectively.

X-ray analysis: The structures were solved by direct methods (SIR-97)^[42] and refined by full-matrix least-squares analysis (SHELXL-97)^[43] using an isotropic extinction correction. All non hydrogen atoms were refined anisotropically; hydrogen atoms were refined isotropically, whereby hydrogen positions are based on stereochemical considerations.

X-ray crystal structure of 1: Crystal data at 220(2) K for C₂₀H₁₁N₇, *M*_r = 349.36, triclinic, space group *P* $\bar{1}$, ρ_{calcd} = 1.278 g cm⁻³, *Z* = 2, *a* = 7.0331(18), *b* = 7.7652(19), *c* = 16.756(2) Å, α = 86.996(14), β = 83.408(15), γ = 88.385(16)°, *V* = 907.6(3) Å³. Bruker–Nonius Kappa-CCD diffractometer, MoK α radiation, λ = 0.7107 Å, μ = 0.082 mm⁻¹. A black crystal of **1** (linear dimensions ca. 0.16 × 0.07 × 0.06 mm) was obtained by slow diffusion of *n*-hexane into a solution of **1** in CH₂Cl₂. Numbers of measured and unique reflections are 3942 and 2466, respectively (*R*_{int} = 0.062). Final *R*(*F*) = 0.072, *wR*(*F*²) = 0.168 for 247 parameters and 1636 reflections with *I* > 2 σ (*I*) and 2.92 < θ < 23.23° (corresponding *R* values based on all 2466 reflections are 0.112 and 0.193, respectively).

X-ray crystal structure of 15: Crystal data at 220(2) K for 2(C₄₆H₂₈N₁₂)-4-(C₂₀H₃₀Fe)-2.5(CH₂Cl₂), *M*_r = 3010.04, monoclinic, space group *P*2₁/*c* (no. 14), ρ_{calcd} = 1.226 g cm⁻³, *Z* = 4, *a* = 21.8649(13), *b* = 31.0432(15), *c* = 26.3554(14) Å, β = 114.293(11)°, *V* = 16305(2) Å³. Bruker–Nonius Kappa-CCD diffractometer, MoK α radiation, λ = 0.7107 Å, μ =

0.489 nm⁻¹. A green crystal of **15** (linear dimensions ca. 0.15 × 0.09 × 0.05 mm) was obtained by slow diffusion of *n*-hexane into a solution of **15** in CH₂Cl₂. Numbers of measured and unique reflections are 33275 and 19452, respectively ($R_{\text{int}}=0.044$). Final $R(F)=0.072$, $wR(F^2)=0.165$ for 1949 parameters and 14056 reflections with $I > 2\sigma(I)$ and $1.66 < \theta < 21.98^\circ$ (corresponding R values based on all 19452 reflections are 0.106 and 0.186, respectively). CCDC-711841 (**1**) and CCDC-711842 (**15**) contain the supplementary crystallographic data for this paper. These data can be obtained free of charge from The Cambridge Crystallographic Data Centre via www.ccdc.cam.ac.uk/data_request/cif.

Silylation of glass surfaces with dimethyldichlorosilane (DMDCS).^[21] The glassware was soaked in a toluene solution of DMDCS (5% v/v) for 15 min at 25 °C. Subsequently, the glassware was rinsed twice with toluene, soaked for 15 min in MeOH, rinsed with MeOH, and finally dried in a nitrogen stream.

3-[(Dicyanomethylidene)-2-[4-(dimethylamino)phenyl]-1,4-pentadiene-1,1,5,5-tetracarboxitrile (1**):** TCNE (48 mg, 0.380 mmol) was added to a solution of **9** (42 mg, 0.190 mmol) in 1,2-dichloroethane (35 mL). The mixture was stirred for 16 h at 60 °C. The solvent was evaporated in vacuo to afford a black solid that was purified by repeated (3 ×) slow diffusion of *n*-hexane into CH₂Cl₂ solution at 25 °C. Subsequent CC (SiO₂, CH₂Cl₂→CH₂Cl₂/EtOAc 95:5; decomp) afforded **1** (17 mg, 26%) as a black metallic-like solid. $R_f=0.48$ (SiO₂, CH₂Cl₂/EtOAc 95:5; decomp); m.p. > 250 °C (decomp); ¹H NMR (500 MHz, CD₂Cl₂): $\delta=3.21$ (s, 6H), 6.80 (d, $J=9.4$ Hz, 2H), 7.67 (d, $J=9.4$ Hz, 2H), 8.02 ppm (s, 1H); ¹³C NMR (125 MHz, CD₂Cl₂): $\delta=40.83, 74.33, 97.59, 100.24, 109.54, 109.82, 110.22, 112.27, 113.36, 114.22, 114.32, 117.29, 132.97, 147.72, 155.16, 155.85, 158.85$ ppm; IR (neat): $\tilde{\nu}=3031$ (w), 2923 (w), 2852 (w), 2214 (s), 1603 (s), 1476 (s), 1457 (s), 1382 (s), 1359 (s), 1275 (m), 1218 (s), 1167 (s), 1059 (m), 943 (m), 898 (w), 825 cm⁻¹ (s); UV/Vis (CH₂Cl₂): $\lambda_{\text{max}}(\epsilon)=317$ (21400), 304 (25000), 486 nm (43300 M⁻¹ cm⁻¹); HR-MALDI-MS (DCTB): m/z calcd for C₂₀H₁₁N₇⁺ [M]⁺: 349.1081; found: 349.1084.

3-[(Dicyanomethylidene)-4-[4-(dimethylamino)phenyl]-1,4-pentadiene-1,1,2,5,5-pentacarboxitrile (2**):** TCNE (13 mg, 0.101 mmol) was added to a solution of **10** (25 mg, 0.101 mmol) in 1,1,2,2-tetrachloroethane (15 mL), and the mixture was stirred for two days at 120 °C. After that time, *n*-hexane (20 mL) was added slowly forming a second layer on the top of the reaction solution and the mixture was allowed to stand for two days at 25 °C. The mother liquor was carefully removed using a Pasteur pipette, and the solid was washed with *n*-hexane. Repeated (3 ×) crystallization by slow diffusion of *n*-hexane into CH₂Cl₂ solution at 25 °C afforded **2** (25 mg, 66%) as a black solid. R_f not determined due to rapid decomposition on SiO₂; m.p. > 232 °C (decomp); ¹H NMR and ¹³C NMR not available due to contamination with paramagnetic species and low solubility of the solid; IR (neat): $\tilde{\nu}=2923$ (w), 2214 (m), 1601 (s), 1485 (s), 1437 (m), 1375 (s), 1191 (s), 1171 (s), 1121 (m), 1064 (w), 941 (w), 822 cm⁻¹ (w); UV/Vis (CH₂Cl₂): $\lambda_{\text{max}}(\epsilon)=295$ (15400), 469 (16300), 657 nm (5600, M⁻¹ cm⁻¹); HR-MALDI-MS (DCTB): m/z calcd for C₂₁H₁₀N₈⁺ [M]⁺: 374.1023; found: 374.1028.

2-[[4-(Dicyanomethylidene)-2,5-cyclohexadien-1-ylidene][4-(dimethylamino)phenyl]methyl]-1,3-butadiene-1,1,4,4-tetracarboxitrile (3**):** TCNQ (92 mg, 0.450 mmol) was added to a solution of **9** (50 mg, 0.226 mmol) in 1,2-dichloroethane (35 mL). The mixture was stirred for five days at 60 °C. The solvent was evaporated in vacuo and the residue purified by repeated (3 ×) slow diffusion of *n*-hexane into CH₂Cl₂ solution at 20 °C. The obtained solid was divided into four portions, which were individually purified by multiple CC (SiO₂, 3 × CH₂Cl₂→CH₂Cl₂/EtOAc 1:1; decomp) to afford **3** (13 mg, 14%) as a deep-blue metallic-like solid. $R_f=0.43$ (SiO₂, CH₂Cl₂/EtOAc 1:1; decomp); m.p. 140–142 °C; ¹H NMR (400 MHz, 1,1,2,2-[D₂]tetrachloroethane): $\delta=3.11$ (s, 6H), 6.70–6.74 (m, 3H), 7.13 (d, $J=9.2$ Hz, 2H), 7.21 (dd, $J=9.5, 1.9$ Hz, 1H), 7.27 (dd, $J=9.5, 1.9$ Hz, 1H), 7.40 (dd, $J=9.5, 1.9$ Hz, 1H), 7.96 ppm (s, 1H); ¹³C NMR (125 MHz, 1,1,2,2-[D₂]tetrachloroethane): $\delta=40.59, 97.26, 98.05, 109.48, 110.49, 110.62, 111.99, 113.40, 114.89, 122.14, 126.21, 126.71, 133.18, 133.29, 135.09, 135.65, 143.32, 151.10, 153.65, 153.77, 161.78$ ppm; IR (neat): $\tilde{\nu}=2857$ (w), 2198 (s), 1607 (w), 1575 (s), 1519 (m), 1395 (m), 1367 (s), 1347 (s), 1162 (s), 1002 (w), 940 (m), 909 (m), 820 cm⁻¹ (m);

UV/Vis (CH₂Cl₂): $\lambda_{\text{max}}(\epsilon)=379$ (sh, 68000), 400 (108400), 633 (13900), 930 nm (1400 M⁻¹ cm⁻¹); HR-MALDI-TOF-MS (TCNQ): m/z calcd for C₂₆H₁₅N₇⁺ [M]⁺: 425.1383; found: 425.1374.

3-[4-(Dicyanomethylidene)-2,3,5,6-tetrafluoro-2,5-cyclohexadien-1-ylidene]-3-[4-(dimethylamino)phenyl]-1-propene-1,1,2-tricarboxitrile (5**):** F₄-TCNQ (57 mg, 0.206 mmol) was added to a solution of **8** (35 mg, 0.206 mmol) in CH₂Cl₂ (50 mL) in a flask deactivated with DMDCS. The mixture was stirred for 17 h at 25 °C. After that time, *n*-hexane (50 mL) was added slowly forming a second layer on the top of the reaction solution and the mixture was allowed to stand for two days at 25 °C. The mother liquor was carefully removed using a Pasteur pipette, and the solid was washed with *n*-hexane. Repeated (3 ×) crystallization by slow diffusion of *n*-hexane into CH₂Cl₂ solution at 25 °C afforded **5** (60 mg, 65%) as a black metallic-like solid. $R_f=0.13$ (SiO₂, CH₂Cl₂/EtOAc 95:5; decomp); m.p. > 410 °C (decomp); ¹H NMR (300 MHz, CD₂Cl₂): $\delta=3.39$ (s, 6H), 6.95 (d, $J=9.4$ Hz, 2H), 7.33 ppm (d, $J=9.4$ Hz, 2H); ¹³C NMR (125 MHz, CD₂Cl₂): not available due to low solubility of the solid; ¹⁹F NMR (282 MHz, CD₂Cl₂): $\delta=-140.53$ (m), -133.24 ppm (brs); IR (neat): $\tilde{\nu}=2652$ (w), 2197 (s), 2181 (m), 1635 (m), 1602 (s), 1532 (m), 1387 (s), 1271 (s), 1200 (s), 1161 (s), 1072 (m), 978 (m), 960 (m), 869 (w), 834 (s), 822 cm⁻¹ (m); UV/Vis (CH₂Cl₂): $\lambda_{\text{max}}(\epsilon)=330$ (12400), 370 (sh, 9300), 391 (12200), 539 (25600), 993 nm (22300 M⁻¹ cm⁻¹); HR-MALDI-TOF-MS (TCNQ): m/z calcd for C₂₃H₁₀N₆F₄⁺ [M]⁺: 446.0898; found: 446.0886; elemental analysis calcd (%) for C₂₃H₁₀N₆F₄ (446.37): C 61.89, H 2.26, N 18.83, F 17.02; found: C 61.92, H 2.43, N 18.65, F 17.12.

2-[[4-(Dicyanomethylidene)-2,3,5,6-tetrafluoro-2,5-cyclohexadien-1-ylidene][4-(dimethylamino)phenyl]methyl]-1,3-butadiene-1,1,4,4-tetracarboxitrile (6**):** F₄-TCNQ (62 mg, 0.225 mmol) was added to a solution of **9** (50 mg, 0.226 mmol) in CH₂Cl₂ (40 mL) in a flask deactivated with DMDCS. The mixture was stirred for 16 h at 25 °C. After that time, *n*-hexane (50 mL) was added and the mixture was allowed to stand for two days at 25 °C. The mother liquor was carefully removed, the solid was washed with *n*-hexane (3 ×) and dried in vacuo to give **6** (94 mg, 84%) as a copper-like solid. $R_f=0.12$ (SiO₂, CH₂Cl₂/EtOAc 95:5; decomp); m.p. > 270 °C (decomp); ¹H NMR, ¹³C NMR, and ¹⁹F NMR not available due to contamination with paramagnetic species and low solubility of the solid; IR (neat): $\tilde{\nu}=3039$ (w), 2925 (w), 2662 (w), 2189 (s), 2162 (s), 1635 (m), 1603 (s), 1505 (s), 1480 (m), 1401 (s), 1357 (s), 1222 (s), 1179 (s), 1079 (m), 1002 (s), 964 (s), 920 (m), 859 (m), 833 cm⁻¹ (s); UV/Vis (CH₂Cl₂): $\lambda_{\text{max}}(\epsilon)=289$ (sh, 20600), 321 (27000), 697 (40600), 942 nm (17000 M⁻¹ cm⁻¹); HR-MALDI-TOF-MS (TCNQ): m/z calcd for C₂₆H₁₁N₇F₄⁺ [M]⁺: 497.1007; found: 497.1019; elemental analysis calcd (%) for C₂₆H₁₁N₇F₄ (497.41): C 62.78, H 2.23, N 19.71, F 15.28; found: C 62.28, H 2.37, N 19.27, F 15.34.

3-[[4-(Dicyanomethylidene)-2,3,5,6-tetrafluoro-2,5-cyclohexadien-1-ylidene][4-(dimethylamino)phenyl]methyl]-1,3-butadiene-1,1,2,4,4-pentacarboxitrile (7**):** F₄-TCNQ (17 mg, 0.061 mmol) was added to a solution of **10** (15 mg, 0.061 mmol) in CH₂Cl₂ (10 mL) in a flask deactivated with DMDCS. The mixture was stirred for five days at 25 °C. After that time, *n*-hexane (10 mL) was added slowly forming a second layer on the top of the reaction solution and the mixture was allowed to stand for three days at 25 °C. The mother liquor was carefully removed using a Pasteur pipette, and the solid was washed with *n*-hexane. Repeated (3 ×) crystallization by slow diffusion of *n*-hexane into CH₂Cl₂ solution at 25 °C afforded **7** (28 mg, 88%) as a black metallic-like solid. R_f not determined due to rapid decomposition on SiO₂; m.p. > 360 °C (decomp); ¹H NMR, ¹³C NMR, and ¹⁹F NMR not available due to contamination with paramagnetic species and low solubility of the solid; IR (neat): $\tilde{\nu}=2196$ (s), 2171 (m), 1633 (m), 1595 (s), 1502 (m), 1476 (m), 1352 (s), 1304 (s), 1200 (s), 1171 (s), 1111 (m), 1030 (m), 972 (m), 869 (w), 836 cm⁻¹ (w); UV/Vis (CH₂Cl₂): $\lambda_{\text{max}}(\epsilon)=306$ (sh, 15900), 342 (19400), 420 (11800), 753 (36700), 1120 nm (9400 M⁻¹ cm⁻¹); HR-MALDI-TOF-MS (TCNQ): m/z calcd for C₂₇H₁₀N₈F₄⁺ [M]⁺: 522.0959; found: 522.0960.

Charge-transfer salt ([FeCp*₂]⁺)₂[12]₂²⁻-1.4 CH₂Cl₂ (15**):** To a solution of **12** (50.0 mg, 0.133 mmol) in dry MeCN (20 mL), [FeCp*₂]⁺ (43.4 mg, 0.133 mmol) in dry CH₂Cl₂ (10 mL) was added dropwise. The originally purple solution became intense green while stirred for 30 min at 25 °C. The solvent was evaporated in vacuo and the dark residue dissolved in

CH₂Cl₂ (15 mL). *n*-Hexane (ca. 15 mL) was added slowly on the top of the CH₂Cl₂ solution forming a second layer, and the mixture was allowed to stand for five days at 0°C. The formed solid was collected by filtration, washed with *n*-hexane, and dried in vacuo (2×10^{-6} mbar) to give an analytical sample of **15** (69.2 mg, 68%) as dark green crystals readily soluble in CH₂Cl₂. Crystals of **15** in equilibrium with the supernatant were used for X-ray crystallographic analysis to prevent loss of co-crystallized solutes. Interestingly, red-brown crystals that were obtained in comparable yields in different runs, featured identical elemental composition and crystallographic parameters as the original sample of **15**. M.p. > 170°C (decomp); IR (neat): $\tilde{\nu}$ = 2961 (w), 2920 (w), 2853 (w), 2796 (w), 2169 (s), 2129 (s), 1601 (s), 1581 (s), 1519 (s), 1476 (m), 1444 (m), 1424 (m), 1338 (s), 1283 (s), 1172 (s), 1124 (m), 1061 (m), 1022 (m), 945 (m), 905 (w), 834 (m), 822 (m), 806 cm⁻¹ (m); IR (CHCl₃): $\tilde{\nu}$ = 3010 (m), 2920 (w), 2868 (w), 2178 (s), 1601 (m), 1582 (s), 1525 (w), 1505 (w), 1477 (w), 1424 (m), 1356 (s), 1334 (s), 1182 (m), 1174 (m), 1022 (m), 989 (w), 946 (w), 904 (w), 839 cm⁻¹ (w); UV/Vis (CH₂Cl₂): λ_{\max} (ϵ) = 277 (52500), 320 (sh, 37700), 437 (33700), 470 (sh, 29000), 620 (39600), 690 (sh, 26000), 1307 nm (28300 M⁻¹cm⁻¹); elemental analysis calcd (%) for C₆₆H₈₈N₁₂Fe₂·1.4 CH₂Cl₂ (1520.29): C 69.05, H 6.02, N 11.06, Cl 6.53; found: C 69.11, H 6.31, N 11.11, Cl 6.54.

Acknowledgement

This research was supported by the ETH Research Council, the NCCR "Nanoscale Science", Basel, and FWF (Austria, project no. P20019). B. E. thanks the "Doktorandinnenkolleg FreChe Materie" for her scholarship. Prof. Dr. P. Walde and Dr. T. Schweizer (ETH Zurich) are gratefully acknowledged for the TGA measurements, and L. Bertschi (ETHZ) for the measurements of the challenging MALDI-TOF spectra. We thank Prof. Dr. J. S. Miller (University of Utah) for many fruitful discussions.

- [1] For selected reviews on cyano-based acceptors, see: a) T. L. Cairns, B. C. McKusick, *Angew. Chem.* **1961**, *73*, 520–525; b) W. R. Hertler, W. Mahler, L. R. Melby, J. S. Miller, R. E. Putscher, O. W. Webster, *Mol. Cryst. Liq. Cryst.* **1989**, *171*, 205–216; c) O. W. Webster, *J. Polym. Sci. Part A: Polym. Chem.* **2002**, *40*, 210–221.
- [2] T. L. Cairns, R. A. Carboni, D. D. Coffman, V. A. Engelhardt, R. E. Heckert, E. L. Little, E. G. McGeer, B. C. McKusick, W. J. Middleton, *J. Am. Chem. Soc.* **1957**, *79*, 2340–2341.
- [3] For selected reviews on the chemistry of TCNE, see: a) A. J. Fatiadi, *Synthesis* **1986**, 249–284; b) A. J. Fatiadi, *Synthesis* **1987**, 749–789; c) A. J. Fatiadi, *Synthesis* **1987**, 959–978; d) J. S. Miller, *Angew. Chem.* **2006**, *118*, 2570–2588; *Angew. Chem. Int. Ed.* **2006**, *45*, 2508–2525.
- [4] a) D. S. Acker, R. J. Harder, W. R. Hertler, W. Mahler, L. R. Melby, R. E. Benson, W. E. Mochel, *J. Am. Chem. Soc.* **1960**, *82*, 6408–6409; b) D. S. Acker, W. R. Hertler, *J. Am. Chem. Soc.* **1962**, *84*, 3370–3374.
- [5] For selected reviews on the chemistry of TCNQ, see: a) B. P. Bespalov, V. V. Titov, *Russ. Chem. Rev.* **1975**, *44*, 1091–1108; b) W. Kaim, M. Moscherosch, *Coord. Chem. Rev.* **1994**, *129*, 157–193.
- [6] a) R. C. Wheland, E. L. Martin, *J. Org. Chem.* **1975**, *40*, 3101–3109; b) N. Martín, J. L. Segura, C. Seoane, *J. Mater. Chem.* **1997**, *7*, 1661–1676; c) S. Hünig, E. Herberth, *Chem. Rev.* **2004**, *104*, 5535–5563; d) R. Gómez, C. Seoane, J. L. Segura, *Chem. Soc. Rev.* **2007**, *36*, 1305–1322.
- [7] For reviews on organic conductors, see: a) Special issue on Molecular Conductors: *Chem. Rev.* **2004**, *104*, 4887–5782, edited by P. Batail; b) T. Otsubo, K. Takimiya, *Bull. Chem. Soc. Jpn.* **2004**, *77*, 43–58; c) G. Saito, Y. Yoshida, *Bull. Chem. Soc. Jpn.* **2007**, *80*, 1–137.
- [8] For some specific references to organic conductors, see: a) J. Ferraris, D. O. Cowan, V. Walatka, Jr., J. H. Perlstein, *J. Am. Chem. Soc.* **1973**, *95*, 948–949; b) R. C. Wheland, J. L. Gillson, *J. Am. Chem. Soc.* **1976**, *98*, 3916–3925; c) T. Imakubo, M. Kibune, H. Yoshino, T. Shirahata, K. Yoza, *J. Mater. Chem.* **2006**, *16*, 4110–4116; d) T. Murata, Y. Morita, Y. Yakiyama, K. Fukui, H. Yamochi, G. Saito, K. Nakasuji, *J. Am. Chem. Soc.* **2007**, *129*, 10837–10846; e) H. Alves, A. S. Molinari, H. Xie, A. F. Morpurgo, *Nat. Mater.* **2008**, *7*, 574–580.
- [9] a) J. S. Miller, J. C. Calabrese, H. Rommelmann, S. R. Chittipeddi, J. H. Zhang, W. M. Reiff, A. J. Epstein, *J. Am. Chem. Soc.* **1987**, *109*, 769–781; b) J. S. Miller, *Inorg. Chem.* **2000**, *39*, 4392–4408; c) J. A. Crayston, J. N. Devine, J. C. Walton, *Tetrahedron* **2000**, *56*, 7829–7857; d) N. Lopez, H. Zhao, A. V. Prosvirin, A. Chouai, M. Shatruck, K. R. Dunbar, *Chem. Commun.* **2007**, 4611–4613.
- [10] a) M. Pfeiffer, K. Leo, X. Zhou, J. S. Huang, M. Hofmann, A. Werner, J. Blochwitz-Nimoth, *Org. Electron.* **2003**, *4*, 89–103; b) K. Walzer, B. Maennig, M. Pfeiffer, K. Leo, *Chem. Rev.* **2007**, *107*, 1233–1271.
- [11] Z. Q. Gao, B. X. Mi, G. Z. Xu, Y. Q. Wan, M. L. Gong, K. W. Cheah, C. H. Chen, *Chem. Commun.* **2008**, 117–119.
- [12] M. I. Bruce, J. R. Rodgers, M. R. Snow, A. G. Swincer, *J. Chem. Soc. Chem. Commun.* **1981**, 271–272.
- [13] For some recent work on TCNE cycloadditions, see: a) Y. Morioka, N. Yoshizawa, J.-i. Nishida, Y. Yamashita, *Chem. Lett.* **2004**, *33*, 1190–1191; b) T. Michinobu, J. C. May, J. H. Lim, C. Boudon, J.-P. Gisselbrecht, P. Seiler, M. Gross, I. Biaggio, F. Diederich, *Chem. Commun.* **2005**, 737–739; c) T. Michinobu, C. Boudon, J.-P. Gisselbrecht, P. Seiler, B. Frank, N. N. P. Moonen, M. Gross, F. Diederich, *Chem. Eur. J.* **2006**, *12*, 1889–1905; d) M. Kivala, C. Boudon, J.-P. Gisselbrecht, P. Seiler, M. Gross, F. Diederich, *Angew. Chem.* **2007**, *119*, 6473–6477; *Angew. Chem. Int. Ed.* **2007**, *46*, 6357–6360; e) J. L. Alonso-Gómez, P. Schanen, P. Rivera-Fuentes, P. Seiler, F. Diederich, *Chem. Eur. J.* **2008**, *14*, 10564–10568; f) J. Xu, X. Liu, J. Lv, M. Zhu, C. Huang, W. Zhou, X. Yin, H. Liu, Y. Li, J. Ye, *Langmuir* **2008**, *24*, 4231–4237; g) T. Shoji, S. Ito, K. Toyota, M. Yasunami, N. Morita, *Chem. Eur. J.* **2008**, *14*, 8398–8408; h) D. J. Armit, M. I. Bruce, B. W. Skelton, A. H. White, *Organometallics* **2008**, *27*, 3556–3563; i) T. Michinobu, *J. Am. Chem. Soc.* **2008**, *130*, 14074–14075.
- [14] K.-i. Onuma, Y. Kai, N. Yasuoka, N. Kasai, *Bull. Chem. Soc. Jpn.* **1975**, *48*, 1696–1700.
- [15] For some recent work on TCNQ cycloadditions, see: a) M. Kivala, C. Boudon, J.-P. Gisselbrecht, P. Seiler, M. Gross, F. Diederich, *Chem. Commun.* **2007**, 4731–4733; b) W. Zhou, J. Xu, H. Zheng, H. Liu, Y. Li, D. Zhu, *J. Org. Chem.* **2008**, *73*, 7702–7709; c) K. Tahara, T. Fujita, M. Sonoda, M. Shiro, Y. Tobe, *J. Am. Chem. Soc.* **2008**, *130*, 14339–14345.
- [16] R. L. Cordiner, M. E. Smith, A. S. Batsanov, D. Albesa-Jové, F. Hartl, J. A. K. Howard, P. J. Low, *Inorg. Chim. Acta* **2006**, *359*, 946–961.
- [17] P. Reutenauer, M. Kivala, P. D. Jarowski, C. Boudon, J.-P. Gisselbrecht, M. Gross, F. Diederich, *Chem. Commun.* **2007**, 4898–4900.
- [18] G. D. McAllister, C. D. Wilfred, R. J. K. Taylor, *Synlett* **2002**, 1291–1292.
- [19] N. N. P. Moonen, W. C. Pomerantz, R. Gist, C. Boudon, J.-P. Gisselbrecht, T. Kawai, A. Kishioka, M. Gross, M. Irie, F. Diederich, *Chem. Eur. J.* **2005**, *11*, 3325–3341. Well-reproducible yields of **10** (19%) were obtained with freshly prepared copper(I) acetate only, see: D. A. Edwards, R. Richards, *J. Chem. Soc. Dalton Trans.* **1973**, 2463–2468.
- [20] N. G. Connelly, W. E. Geiger, *Chem. Rev.* **1996**, *96*, 877–910.
- [21] F. Deyhimi, J. A. Coles, *Helv. Chim. Acta* **1982**, *65*, 1752–1759.
- [22] C. Dehu, F. Meyers, J. L. Brédas, *J. Am. Chem. Soc.* **1993**, *115*, 6198–6206.
- [23] For examples of organic molecules with exceptionally small HOMO–LUMO gaps, see: a) A. Tsuda, A. Osuka, *Adv. Mater.* **2002**, *14*, 75–79; b) D. Bonifazi, G. Accorsi, N. Armaroli, F. Song, A. Palkar, L. Echegoyen, M. Scholl, P. Seiler, B. Jaun, F. Diederich, *Helv. Chim. Acta* **2005**, *88*, 1839–1884; c) D. F. Perepichka, M. R. Bryce, *Angew. Chem.* **2005**, *117*, 5504–5507; *Angew. Chem. Int. Ed.* **2005**, *44*, 5370–5373.
- [24] F. Neese, *J. Chem. Phys.* **2003**, *119*, 9428–9443.

- [25] F. Neese, ORCA—An ab initio, DFT, and semiempirical SCF-MO package, Version 2.5, revision 20 (29.01.2007), Max Planck Institute für Strahlenchemie, Mülheim, **2003**.
- [26] C. Diaz, A. Arancibia, *Polyhedron* **2000**, *19*, 137–145.
- [27] Comparable anodic shifts were observed upon CN-substitution in porphyrins, see: a) A. Giraudeau, I. Ezahr, M. Gross, H. J. Callot, J. Jordan, *Bioelectrochem. Bioenerg.* **1976**, *3*, 519–527; b) H. J. Callot, A. Giraudeau, M. Gross, *J. Chem. Soc. Perkin Trans. 2* **1975**, 1321–1324.
- [28] For redox properties of TCNQ vs. F₄-TCNQ, see: A. F. Garito, A. J. Heeger, *Acc. Chem. Res.* **1974**, *7*, 232–240.
- [29] C. Hansch, A. Leo, R. W. Taft, *Chem. Rev.* **1991**, *91*, 165–195.
- [30] A. Klamt, G. Schüürmann, *J. Chem. Soc. Perkin Trans. 2* **1993**, 799–805.
- [31] The calculated EA for F₄-TCNQ (4.96 eV) using the BP86/def-TZVP COSMO($\epsilon=4.5$)/BP86/def-SV(P) method is in good agreement with the reported value obtained experimentally (5.24 eV) by inverse photoemission spectroscopy (IPES). For the experimental EA of F₄-TCNQ, see: W. Gao, A. Kahn, *Appl. Phys. Lett.* **2001**, *79*, 4040–4042.
- [32] a) W. D. Phillips, J. C. Rowell, S. I. Weissman, *J. Chem. Phys.* **1960**, *33*, 626–627; b) F. Gerson, R. Heckendorn, D. O. Cowan, A. M. Kini, M. Maxfield, *J. Am. Chem. Soc.* **1983**, *105*, 7017–7023.
- [33] For selected examples of TCNQ σ -dimers, see: a) V. Dong, H. Endres, H. J. Keller, W. Moroni, D. Nöthe, *Acta. Crystallogr. Sect. B.* **1977**, *33*, 2428–2431; b) B. Morosin, H. J. Plastas, L. B. Coleman, J. M. Stewart, *Acta. Crystallogr. Sect. B.* **1978**, *34*, 540–543; c) S. K. Hoffmann, P. J. Corvan, P. Singh, C. N. Sethulekshmi, R. M. Metzger, W. E. Hatfield, *J. Am. Chem. Soc.* **1983**, *105*, 4608–4617; d) H. Zhao, R. A. Heintz, K. R. Dunbar, *J. Am. Chem. Soc.* **1996**, *118*, 12844–12845; e) S. Mikami, K.-i. Sugiura, J. S. Miller, Y. Sakata, *Chem. Lett.* **1999**, 413–414; f) C. Alonso, L. Ballester, A. Gutiérrez, M. F. Perpiñán, A. E. Sánchez, M. T. Azcondo, *Eur. J. Inorg. Chem.* **2005**, 486–495; g) S. Shimomura, S. Horike, R. Matsuda, S. Kitagawa, *J. Am. Chem. Soc.* **2007**, *129*, 10990–10991.
- [34] The estimated standard deviations (ESDs) from least squares refinement are nearly the same for both independent [12]₂²⁻ molecules (**A** and **B**) and range from 0.004 to 0.006 Å. For the three ordered [FeCp*₂]⁺ molecules, the ESDs for Fe–C and C–C bond lengths range from 0.003 to 0.005 Å and from 0.004 to 0.007 Å, respectively. The experimental bond lengths correspond to the average of both independent [12]₂²⁻ molecules **A** and **B**.
- [35] a) M. Decoster, F. Conan, M. Kubicki, Y. Le Mest, P. Richard, J. S. Pala, L. Toupet, *J. Chem. Soc. Perkin Trans. 2* **1997**, 265–271; b) S. Duclos, F. Conan, S. Triki, Y. Le Mest, M. L. Gonzales, J. S. Pala, *Polyhedron* **1999**, *18*, 1935–1939.
- [36] Gaussian 03, Revision C.02, M. J. Frisch, G. W. Trucks, H. B. Schlegel, G. E. Scuseria, M. A. Robb, J. R. Cheeseman, J. Montgomery, Jr., T. Vreven, K. N. Kudin, J. C. Burant, J. M. Millam, S. S. Iyengar, J. Tomasi, V. Barone, B. Mennucci, M. Cossi, G. Scalmani, N. Rega, G. A. Petersson, H. Nakatsuji, M. Hada, M. Ehara, K. Toyota, R. Fukuda, J. Hasegawa, M. Ishida, T. Nakajima, Y. Honda, O. Kitao, H. Nakai, M. Klene, X. Li, J. E. Knox, H. P. Hratchian, J. B. Cross, C. Adamo, V. Bakken, C. Adamo, J. Jaramillo, R. Gomperts, R. E. Stratmann, O. Yazyev, A. J. Austin, R. Cammi, C. Pomelli, J. W. Ochterski, P. Y. Ayala, K. Morokuma, G. A. Voth, P. Salvador, J. J. Dannenberg, V. G. Zakrzewski, S. Dapprich, A. D. Daniels, M. C. Strain, O. Farkas, D. K. Malick, A. D. Rabuck, K. Raghavachari, J. B. Foresman, J. V. Ortiz, Q. Cui, A. G. Baboul, S. Clifford, J. Cioslowski, B. B. Stefanov, G. Liu, A. Liashenko, P. Piskorz, I. Komaromi, R. L. Martin, D. J. Fox, T. Keith, M. A. Al-Laham, C. Y. Peng, A. Nanayakkara, M. Challacombe, P. M. W. Gill, B. Johnson, W. Chen, M. W. Wong, C. Gonzalez, J. A. Pople, Gaussian, Inc., Wallingford CT, **2004**.
- [37] A. H. Reis, Jr., L. D. Preston, J. M. Williams, S. W. Peterson, G. A. Candela, L. J. Swartzendruber, J. S. Miller, *J. Am. Chem. Soc.* **1979**, *101*, 2756–2758.
- [38] a) J.-M. Lü, S. V. Rosokha, J. K. Kochi, *J. Am. Chem. Soc.* **2003**, *125*, 12161–12171; b) T. Nishinaga, K. Komatsu, *Org. Biomol. Chem.* **2005**, *3*, 561–569.
- [39] a) H. Zhao, R. A. Heintz, X. Ouyang, K. R. Dunbar, C. F. Campana, R. D. Rogers, *Chem. Mater.* **1999**, *11*, 736–746; b) L. Ballester, A. Gutiérrez, M. F. Perpiñán, M. T. Azcondo, A. E. Sánchez, *Synth. Met.* **2001**, *120*, 965–966.
- [40] Electronic Structure Calculations on Workstation Computers: The Program System TURBOMOLE, see: R. Ahlrichs, M. Bär, M. Häser, H. Horn, C. Kölmel, *Chem. Phys. Lett.* **1989**, *162*, 165–169.
- [41] A. Schäfer, C. Huber, R. Ahlrichs, *J. Chem. Phys.* **1994**, *100*, 5829–5835.
- [42] A. Altomare, M. C. Burla, M. Camalli, G. L. Cascarano, C. Giacovazzo, A. Guagliardi, A. G. G. Moliterni, G. Polidori, R. Spagna, *J. Appl. Crystallogr.* **1999**, *32*, 115–119.
- [43] G. M. Sheldrick, SHELXL-97, Program for the Refinement of Crystal Structures, University of Göttingen, Germany, **1997**.

Received: December 6, 2008
Published online: March 5, 2009